

Coherent States and Modified de Broglie-Bohm Complex Quantum Trajectories

Moncy V. John · Kiran Mathew

Received: 12 November 2012 / Accepted: 29 May 2013 / Published online: 14 June 2013
© Springer Science+Business Media New York 2013

Abstract This paper examines the nature of classical correspondence in the case of coherent states at the level of quantum trajectories. We first show that for a harmonic oscillator, the coherent state complex quantum trajectories and the complex classical trajectories are identical to each other. This congruence in the complex plane, not restricted to high quantum numbers alone, illustrates that the harmonic oscillator in a coherent state executes classical motion. The quantum trajectories we consider are those conceived in a modified de Broglie-Bohm scheme. Though quantum trajectory representations are widely discussed in recent years, identical classical and quantum trajectories for coherent states are obtained only in the present approach. We may note that this result for standard harmonic oscillator coherent states is not totally unexpected because of their holomorphic nature. The study is extended to coherent states of a particle in an infinite potential well and that in a symmetric Poschl-Teller potential by solving for the trajectories numerically. For the Gazeau-Klauder coherent state of the infinite potential well, almost identical classical and quantum trajectories are obtained whereas for the Poschl-Teller potential, though classical trajectories are not regained, a periodic motion results as $t \rightarrow \infty$. Similar features were found for the SUSY quantum mechanics-based coherent states of the Poschl-Teller potential too, but this time the pattern of complex trajectories is quite different from that of the previous case. Thus we find that the method is a potential tool in analyzing the properties of generalized coherent states.

Keywords Quantum trajectory · Coherent state · Classical correspondence

M.V. John (✉) · K. Mathew
Department of Physics, St. Thomas College, Kozhencherri 689641, Kerala, India
e-mail: moncyjohn@yahoo.co.uk

K. Mathew
e-mail: kiran007x@yahoo.co.in

1 Introduction

Quantum trajectories, such as those due to de Broglie and Bohm (dBB), Floyd, Faraggi and Matone (FFM), etc., have gained wide attention [1–10] recently. In another attempt, complex quantum trajectories were conceived by a modified de Broglie-Bohm (MdBB) approach to quantum mechanics [11–22]. These trajectories are obtained by putting $\Psi \equiv \exp(iS/\hbar)$ in the Schrodinger equation, which results in an equation similar to the classical Hamilton-Jacobi equation, in terms of the generally complex function $S(x, t)$. Instead of using the Hamilton-Jacobi formalism (where one must use the Jacobi's theorem to obtain trajectories, as in classical mechanics and the FFM trajectory representation [9, 10]), an equation of motion [11]

$$\dot{x} = \frac{1}{m} \nabla S, \quad (1)$$

is used, where x now is a complex variable $x \equiv x_r + ix_i$. This equation appears similar to but is not the same as that used by de Broglie [1–3] to obtain a velocity field. On integration, it gives complex trajectories, in contrast to the real trajectories in the dBB approach.

Our attempt in this paper is to find the nature of classical correspondence at the level of quantum trajectories of particles in coherent states [23, 24] (denoted as $\phi_z(x, t)$, where z is a complex parameter), moving in potentials such as the harmonic oscillator, infinite potential well, a symmetric Poschl-Teller potential etc. It is found that the MdBB representation has the feature of identical classical and quantum trajectories for harmonic oscillator coherent states. For the coherent state of the infinite potential well, one can observe this feature in the limit of high $|z|$. But for the Poschl-Teller potential, such a conclusion cannot be made. However, periodic motion for the particle results as $t \rightarrow \infty$ for both the Gazeau-Klauder coherent states and the supersymmetric quantum mechanics (SUSYQM)-based coherent states.

Since the MdBB quantum trajectories are in a complex plane, the demonstration of identical quantum and classical trajectories is to be made in the complex plane. The theory of coherent states is inextricably connected to the complex parameter z and hence identical trajectories for the quantum and classical cases in the complex space is not unnatural.

Given below, in Fig. 1, are the trajectories for the quantum harmonic oscillator in the lowest energy eigenstates with $n = 0, 1, 2, 3$ and 4, drawn using numerical methods. Similarly, in Fig. 2, the corresponding complex quantum trajectories for a particle in an infinite potential well are drawn numerically. Such solutions for these stationary states agree very well with the analytical solutions in [11, 14]. They serve as benchmark for the numerical method and encourages us to apply it to other problems with known wave functions as well.

2 Complex Classical Trajectories

Solutions of classical dynamical problems of physical systems obtained in terms of complex space variables are well-known. In the past decade, interesting properties

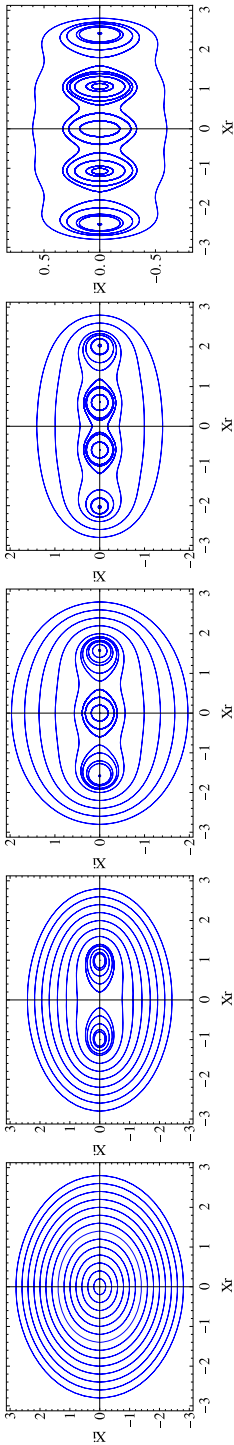


Fig. 1 The complex quantum trajectories for the harmonic oscillator in the $n = 0, 1, 2, 3, 4$ energy eigenstates, respectively, for evenly distributed starting points along the real line

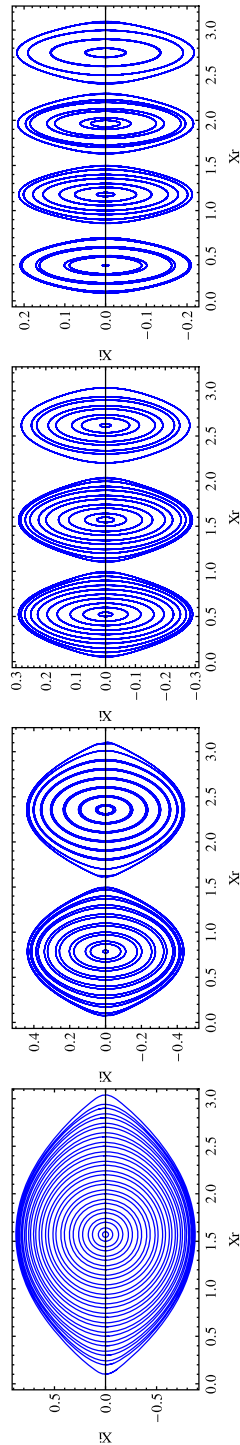
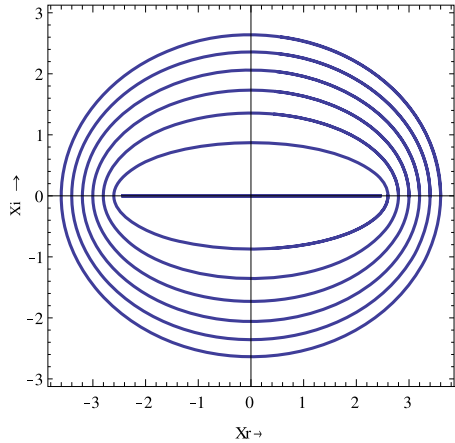


Fig. 2 The complex quantum trajectories for the particle in an infinite well potential in the $n = 0, 1, 2, 3$ energy eigenstates, respectively, for evenly distributed starting points along the real line

Fig. 3 The complex classical trajectories for the harmonic oscillator of energy $E = 4.5$ units



of classical trajectories of complex Hamiltonians are discovered [25–27]. To obtain complex trajectories, one solves the Hamilton’s equations $\dot{x} = \frac{\partial H}{\partial p}$, $\dot{p} = -\frac{\partial H}{\partial x}$, for complex initial conditions and not just for initial conditions in the classically allowed regions. For instance, consider the harmonic oscillator problem. With $H = p^2/2m + (1/2)kx^2$, $x \equiv x_r + ix_i$, and the complex momentum $p \equiv p_r + ip_i$, one writes the Hamilton’s equations as $\dot{x}_r = p_r/m$, $\dot{x}_i = p_i/m$, $\dot{p}_r = -kx_r$ and $\dot{p}_i = -kx_i$. For a particle with real energy E such that $0 < E < (1/2)kA^2 = (1/2)m\omega^2A^2$, the solution of these equations can be found as

$$x_r = A \cos(\omega t), \quad x_i = B \sin(\omega t), \quad B = \sqrt{A^2 - \frac{2E}{m\omega^2}}. \tag{2}$$

This leads to elliptical trajectories in the complex plane, as plotted in Fig. 3. Note that in the limit $E \rightarrow 0$, these ellipses become concentric circles.

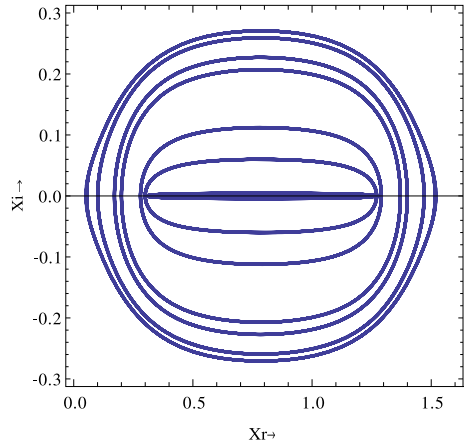
Now consider the case of a free particle with real energy $E > 0$. Then we have $\dot{x}_r = p_r/m$, $\dot{x}_i = p_i/m$, $\dot{p}_r = 0$, $\dot{p}_i = 0$, $p_r p_i = 0$ and also $p_r^2 > p_i^2$. Then the solutions are $x_r = \pm\sqrt{\frac{2E}{m}}t + c_r$, $x_i = c_i$, where the constants c_r , c_i are real. These classical trajectories are straight lines which lie in the complex plane, parallel to the real axis.

Another example we consider here is that of a Poschl-Teller potential

$$V(x) = \frac{V_0}{2} \left[\frac{l(l-1)}{\cos^2(\frac{x}{2a})} + \frac{k(k-1)}{\sin^2(\frac{x}{2a})} \right]. \tag{3}$$

The symmetric Poschl-Teller potential results when we take $l = k \geq 1$ [28]. Putting $2a$ to be of unit magnitude, the potential becomes $V(x) = 2V_0l(l-1)/\sin^2(2x)$. The complex classical trajectories for a particle having an energy $E = 2.25$ units are drawn numerically in Fig. 4.

Fig. 4 The complex classical trajectories for a particle with $E = 2.25$ units in the symmetric Poschl-Teller potential



3 Complex Quantum Trajectories of Harmonic Oscillator Coherent States

We may now illustrate that the complex quantum trajectories of the harmonic oscillator in coherent state are the same as those trajectories obtained in complex classical mechanics. Here it is shown that these are identical to each other for all mean values of energy, thus demonstrating the quantum-classical correspondence. We start with the coherent state wave function of a harmonic oscillator with $X \equiv \alpha x$,

$$\phi_z(x, t) = \left(\frac{\alpha}{\sqrt{\pi}}\right)^{1/2} \exp\left[\frac{1}{2}(X^2 - \lambda^2 - i\omega t)\right] \exp[-(X - \eta)^2], \tag{4}$$

where $\alpha = \sqrt{m\omega/\hbar}$, $z = \lambda e^{i\kappa}$, and $\eta = \frac{1}{\sqrt{2}}\lambda e^{-i(\omega t - \kappa)}$. The de Broglie-type equation of motion used in MdBB [11] gives

$$\dot{X} = i\omega(X - 2\eta). \tag{5}$$

The above coherent state ϕ_z is the eigenfunction of the lowering operator a with eigenvalue z , which is complex. Note that in the limit $\lambda \rightarrow 0$, the coherent state wave function and its equation of motion reduce to the corresponding entities of harmonic oscillator ground state, as expected. The real and imaginary parts of the velocity field \dot{X} are

$$\dot{X}_r = -\omega[X_i + \sqrt{2}\lambda \sin(\omega t - \kappa)] \tag{6}$$

and

$$\dot{X}_i = \omega[X_r - \sqrt{2}\lambda \cos(\omega t - \kappa)]. \tag{7}$$

These equations have the solutions $X_r = A \cos(\omega t - \kappa)$ and $X_i = B \sin(\omega t - \kappa)$, which are the same as the solutions of the classical Hamilton’s equations obtained in (2), except for a phase factor, when A, B (both real and positive) are related to λ by the equation $A - B = \sqrt{2}\lambda$. Each one of such quantum trajectories in MdBB corresponds to a trajectory of the complex classical oscillator. This congruence establishes the correspondence of a quantum harmonic oscillator in coherent state with the

classical harmonic oscillator. In the limit $\lambda \rightarrow 0$, the solution with $A = B$ exists. This gives concentric circular paths corresponding to the ground state harmonic oscillator obtained in [11, 14].

Let us now compare the coherent state MdBB trajectories for the harmonic oscillator with those in the dBB guiding wave mechanics. The equation of motion in the latter case is $\dot{X} = -\omega\sqrt{2}\lambda \sin(\omega t - \kappa)$, with X real. The trajectories are non-crossing [5] and the particles oscillate with amplitude $A = \sqrt{2}\lambda$. In the limit $\lambda \rightarrow 0$ (which is equivalent to the condition that the mean value of energy $E \rightarrow 0$), they remain stationary at their initial positions $X(0)$. We note that in the real case, classical simple harmonic oscillators can, at best, be stationary only at the equilibrium point $X = 0$ and that the above feature of stationary particles at all values of X is unnatural in the classical limit. On the other hand, the MdBB trajectories in the coherent state correspond to the complex classical trajectories in every respect. Even for $\lambda \rightarrow 0$, all the trajectories enclose $X = 0$; they are concentric circles of the $n = 0$ harmonic oscillator state given in Fig. 1 and agree with the corresponding classical trajectories. Often in conventional dBB scheme, the stationarity of particles in bound eigenstates is justified as an instance which demands a new ‘quantum intuition’, but the above mentioned failure to exhibit correspondence with classical motion, even for coherent states, is indeed a setback for the formalism.

By using numerical methods the complex trajectories for the harmonic oscillator in a coherent state with $|z| = \lambda = 2.1$ are drawn. Instead of expression (4), we use the expansion

$$\phi_z(x, t) = \sum_{n \geq 0} e^{-\frac{1}{2}|z|^2} \frac{z^n}{\sqrt{n!}} e^{-i(n+\frac{1}{2})\omega t} \psi_n(x) \quad (8)$$

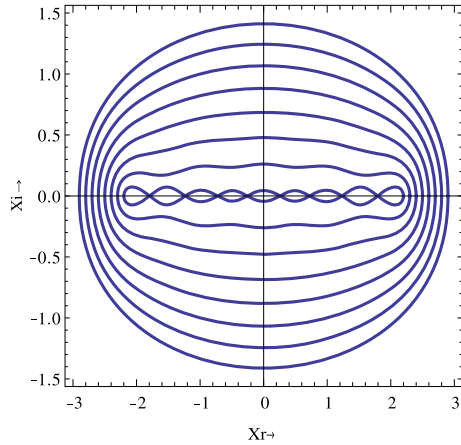
for obtaining the coherent states in terms of the eigenfunctions. The trajectories are shown in Fig. 5. In this numerical evaluation, we have included terms up to $n = 4$ in the expansion. One finds deviations from the expected classical trajectories at the inner parts. It can easily be seen that those trajectories with large values of $x(0)$ are almost circular in shape and they always agree with the complex classical trajectories. When the number of terms included in the series is varied, however, the shape of trajectories at the inner regions, with small values of $x(0)$, vary significantly. The deviations of these trajectories with those drawn using Eqs. (6) and (7) are thus expected to arise from the truncation in the series.

4 Infinite Potential Well and Poschl-Teller Potential

As another example, now consider a particle of mass m and energy E , trapped in an infinite potential well of width πa . As seen in Sect. 3, the classical trajectories are straight lines in the complex plane, lying parallel to the real axis. Let us attempt to solve the quantum problem with a shifted Hamiltonian [28]

$$H = -\frac{\hbar^2}{2m} \frac{d^2}{dx^2} - \frac{\hbar^2}{2ma^2}, \quad (9)$$

Fig. 5 The complex trajectories for the harmonic oscillator in a coherent state with $\lambda = 2.1$ and $\kappa = 0$, evaluated numerically by including terms up to $n = 4$ in the expansion. The trajectories are plotted for the initial values $x_r = 2.2, 2.3, 2.4, 2.5, 2.6, 2.7, 2.8$ and 2.9



together with the boundary condition

$$\psi(x) = 0, \quad x \geq \pi a \quad \text{and} \quad x \leq 0. \tag{10}$$

The normalized eigenstates and corresponding eigenvalues are

$$\psi_n(x) = \sqrt{\frac{2}{\pi a}} \sin(n + 1) \frac{x}{a}, \quad n = 0, 1, \dots \tag{11}$$

and

$$E_n = \hbar\omega e_n, \tag{12}$$

with

$$\omega = \frac{\hbar}{2ma^2} \quad \text{and} \quad e_n = n(n + 2), \quad n = 0, 1, \dots \tag{13}$$

With $a = 1$, we have drawn the complex quantum trajectories corresponding to $n = 0, 1, 2, 3, 4$ states of the infinite potential well eigenstates in Fig. 2. The coherent states of this particle can be written as [28]

$$\phi_J(x, t) = \frac{1}{N(J)} \sum_{n \geq 0} \frac{J^{n/2}}{\sqrt{\frac{n!(n+2)!}{2}}} e^{-in(n+2)\omega t} \psi_n(x). \tag{14}$$

The numerically evaluated complex trajectories for the particle in the $J = 0.04, 0.16, 0.25, 0.36$ coherent states, with $\omega = 1$, are shown in Fig. 6. In this numerical approach, we have included terms up to $n = 7$ in the expansion (14). It is interesting to note the presence of almost straight trajectories parallel to the real axis, as in the case of classical complex trajectory solutions of free particles (Sect. 2). But near the turning points, the trajectories are more like those near the turning points of classical symmetric Poschl-Teller potentials. In this case, deviations from the classically expected straight line trajectories (mentioned above) at the inner region do not seem to arise from truncation errors in the numerical method. This can be seen by varying

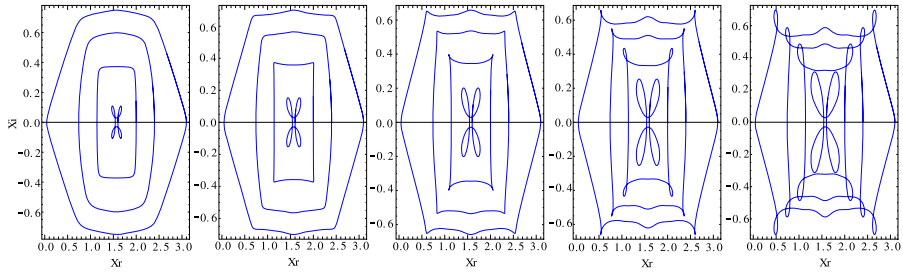


Fig. 6 The numerically evaluated complex trajectories for the particle in coherent state in an infinite well potential, in the $J = 0.04, 0.09, 0.16, 0.25, 0.36$ cases. In all cases, trajectories are plotted for the initial values of $x_r = 1.6, 2.0, 2.4$ and 3.1 , respectively

the number of terms in the series (14). The curves are the same even if we include only terms up to $n = 4$. But drawing trajectories for much larger values of J than that given in Fig. 6 is not possible with the present numerical method. For such values of J , the trajectories are not confined to the physically limited interval of $0 < x_r < \pi$ while using this method.

The next problem we consider is the symmetric Poschl-Teller potential

$$V(x) = 2V_0 \frac{l(l-1)}{\sin^2(2x)}, \tag{15}$$

whose classical trajectories are discussed in Sect. 3. We have taken $l = k$ and $2a = 1$ in Eq. (3). In addition, we consider a shifted Hamiltonian [28]

$$H = -\frac{\hbar^2}{2m} \frac{d^2}{dx^2} - 2\frac{\hbar^2}{m} l^2 + V(x). \tag{16}$$

Solving the Schrodinger equation with the boundary condition $\psi(0) = \psi(\pi/2) = 0$, the normalized eigenstates can be found as

$$\psi_n(x) = [c_n(l)]^{-1/2} \cos^l(x) \sin^l(x) {}_2F_1(-n, n + 2l; l + (1/2); \sin^2 x). \tag{17}$$

Here we choose $l = 3/2$. The Gazeau-Klauder coherent states are [28]

$$\phi_J(x, t) = \frac{\sqrt{3!}}{N(J)} \sum_{n \geq 0} \frac{J^{n/2}}{\sqrt{n!(n+3)!}} e^{-in(n+3)\omega t} \psi_n(x), \tag{18}$$

where $\omega = \hbar/2ma^2$. The complex quantum trajectories, evaluated numerically with $\omega = 1$, a value of $J = 0.16$ and for different initial points are shown in Fig. 7. Terms up to $n = 4$ are included in the series.

These trajectories are not identical to those of the corresponding classical case; i.e., there is no congruence with the classical trajectories in this case. However, some interesting features of these trajectories may be noted. First, for initial points close to the boundary of the potential, they spiral inwards with a period; i.e., the maximum displacements from the center to either side on the real and imaginary axes decrease

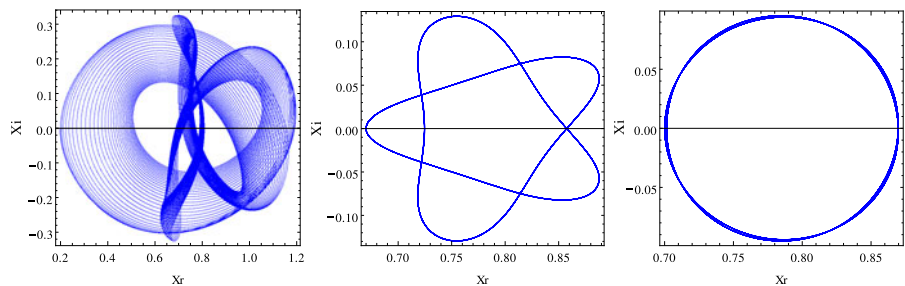


Fig. 7 The complex trajectories for the particle in a Gazeau-Klauder coherent state with $J = 0.16$ in the Poschl-Teller potential. The trajectories in different plots are for the initial values on the real line $x_{r0} = 0.2, 0.67, 0.7015$ respectively and for $0 < t < 100$ in each case

with each cycle. This can be seen clearly from the first trajectory in Fig. 7, which has starting point $x_{r0} = 0.2$. When the initial point is nearer to the bottom of the potential, such as $x_{r0} = 0.67$ shown in the second figure, we have a pentagonal star-shaped trajectory. The point $x_{r0} = 0.7015$ is special for the case of $J = 0.16$, since it leads to an almost circular trajectory in the complex plane and the particle remains in it for ever. It is interesting to note that if we follow the trajectory for large t , the pattern evolves with time and passes through these different phases. Thus the trajectory in the third panel is the final one, in the limit $t \rightarrow \infty$, for whatever initial point one starts with. In particular, we have observed that the trajectory with the initial point $x_{r0} = 0.2$, drawn in Fig. 7, approaches this final shape asymptotically. During this process, also its orientation changed from anti-clockwise to clockwise and period changed from π to $\pi/2$. Including only terms up to $n = 3$ does not significantly affect the shape of this or neighboring trajectories. Hence we conclude that also in Fig. 7, the shape of the trajectories do not arise from truncation errors. For values of J much larger than that in this figure, the trajectories cannot be drawn since they are not confined to the physically limited interval of $0 < x_r < \pi/2$. This may be due to the error in truncation.

There is another class of coherent states based on supersymmetric quantum mechanics (SUSYQM) [29, 30]. In the case of symmetric Poschl-Teller potential given in Eq. (15), let us take $V_0 = \hbar^2/m$ and keep the Hamiltonian as

$$H_l = -\frac{\hbar^2}{2m} \frac{d^2}{dx^2} + \frac{2\hbar^2}{m} \frac{l(l-1)}{\sin^2(2x)}. \tag{19}$$

Then the energy eigenvalues can be written as

$$E_n = \frac{2\hbar^2}{m} (n+l)^2, \tag{20}$$

while the eigenstates $\psi_n(x)$ are the same as that in Eq. (17).

The superpotential $W_l(x)$ in this case are defined as $W_l(x) = -2\hbar l \cot(2x)$ [29, 30] and the lowering and raising operators A_l and A_l^\dagger are, respectively,

$$A_l \equiv W_l + \hbar \frac{d}{dx} \quad \text{and} \quad A_l^\dagger \equiv W_l - \hbar \frac{d}{dx}. \tag{21}$$

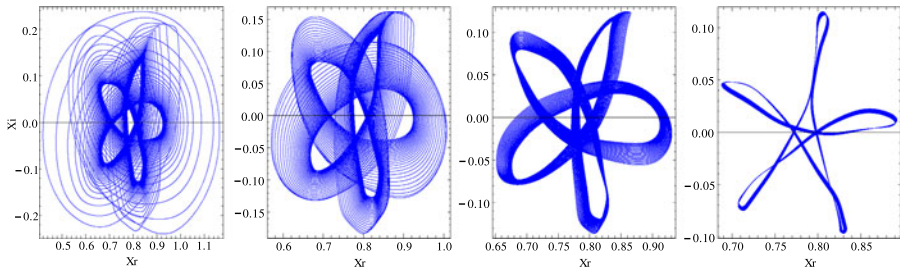


Fig. 8 The complex trajectories for the particle in a SUSYQM coherent state with $q = 0.8$ and $k = 0.5$ in the Pöschl-Teller potential. The trajectories in the different plots are for the initial values on the real line $x_{r0} = 0.55, 0.65, 0.72, \pi/4$, respectively and for $0 < t < 100$ in each case

The Hamiltonian H_l now becomes $H_l = \frac{1}{2m} A_l^\dagger A_l + E_0$. The SUSYQM coherent states are the normalized eigenvectors of A_l and can be written as

$$\eta_{q,k}(x) = N(q)e^{(-3 \cot(2q) + ik)x} \sin^{3/2}(2x), \tag{22}$$

where we have taken $l = 3/2$ as in the previous case of Gazeau-Klauder coherent states. The corresponding eigenvalues are $-3\hbar \cot(2q) + i\hbar k$. The time evolution of this state can be found using the usual approach of expanding $\eta_{q,k}(x, t)$ in terms of the eigenfunctions $\psi_n(x)$ given in Eq. (17):

$$\eta_{q,k}(x, t) = \sum_{n=0}^{\infty} a_n \psi_n(x) e^{-i \frac{E_n}{\hbar} t} = \sum_{n=0}^{\infty} c_n \psi_n(x) e^{-i(n + \frac{3}{2})^2 \omega t} \tag{23}$$

where $\omega = 2\hbar/m$ in this case. Then the coefficients a_n can be found as

$$a_n = \int_0^{\pi/2} \psi_n^*(x) \eta_{q,k}(x, 0) dx.$$

Putting $q = 0.8$ and $k = 0.5$, the values obtained numerically for the first few of these coefficients are $a_0 = 0.80121555 + i 0.33440120$, $a_1 = 0.02393104 - i 0.10634033$, $a_2 = -0.00838162 - i 0.00039834$, $a_3 = 0.00168689 - i 0.00677396$, $a_4 = -0.00133694 - i 0.00007039$, $a_5 = 0.00041423 - i 0.00164860$. Using these in Eq. (23), complex quantum trajectories were drawn for various initial values, following the numerical method adopted in the previous cases. Figure 8 shows such trajectories for initial values $x_{r0} = 0.55, 0.65, 0.72$, and $\pi/4$, respectively. It was found that the situation is similar to that of the Gazeau-Klauder coherent states for the same potential, but has quite different patterns for the complex trajectories. Trajectories which start from points away from the minimum of the potential ($x_r = \pi/4$) can be seen to inspiral as in the previous case, but they appear to be more symmetrical (For example, see the first two diagrams in the panel of Fig. 8). Similarly for points close to the minimum of the potential (for instance, $x_{r0} = 0.72$), the pattern evolves to that of a pentagonal flower. Moreover, the final temporally stable pattern (the last one in Fig. 8, where $x_{r0} = \pi/4$) is not a circle, which demonstrates that this SUSYQM coherent state is quite distinct from Gazeau-Klauder coherent states.

We have attempted to draw these trajectories for various combinations of the values of q , k and starting points x_{r0} . In all cases, the shape of trajectories remain the same. However, it was not possible to draw the trajectories for values of both q and starting points near the turning points and $k \gg 1$, possibly due to truncation errors. In such cases, the trajectories were not found confined to the physically limited interval of $0 < x_r < \pi/2$.

5 Conclusion

Using the MdBb approach, we have illustrated that the coherent state trajectories of the harmonic oscillator are identical to the complex classical trajectories. This feature is not restricted to high energies alone. We note that this result is not totally unexpected for standard coherent states because of their holomorphic nature. However, such congruence is as yet reported only in the MdBb quantum trajectory representation. The analysis is extended to potentials such as an infinite well and a symmetric Pöschl-Teller potential. We have used numerical methods for the plotting of complex trajectories in such cases. It is found that for a particle trapped in an infinite potential well, the coherent state complex trajectories partly agree with the classical solutions. For large values of the parameter J , the agreement becomes almost perfect when initial points are located close to the turning points. On the other hand, for the Pöschl-Teller potential, no congruence is observed and hence no exact classical correspondence can be claimed for both Gazeau-Klauder and SUSYQM coherent states. But we find that the complex trajectories of these coherent states become periodic as $t \rightarrow \infty$, for typical values of the parameters involved. Most interestingly, different generalized coherent states have different complex trajectories with distinguishable patterns.

There were several attempts to formulate complex quantum mechanics, such as that in [31] and references therein, where complex space variables appear. But they are not directly related to the de Broglie-Bohm quantum trajectories approach and does not envisage individual particle trajectories as in Bohmian mechanics. However, it remains a strong possibility that such works on complex quantum mechanics shall be of help to explain, in a more comprehensive way, the physical interests behind the present work. In this paper, our attempt is to see whether the complex classical trajectories of particles [25–27] in various potentials are identical to the complex trajectories in a modified version of de Broglie-Bohm quantum theory, for the corresponding coherent states. Since this is our main concern, other complex formulations of quantum mechanics are not considered here. But we wish to highlight that to proceed further, the complex quantum mechanics developed in the above references can be of immense help.

Exploring the classical correspondence of coherent states at the level of quantum trajectories is capable of revealing more information on the fundamental nature of coherent states. It is interesting to note how the individual eigenstates which lead to trajectories in Fig. 2 combine to form a coherent state with quantum trajectories shown in Fig. 6, that at least partly agree with the classical solutions. Similarly, the eigenstates of Pöschl-Teller potential combine to form coherent states having trajectories that correspond to periodic classical trajectories. In general, such trajectories

have very interesting properties, which makes the method a potential tool in analyzing the properties of generalized coherent states.

Acknowledgements M.V.J. wishes to thank Professors N.D. Hari Dass and M. Raveendranadhan for discussions and the Chennai Mathematical Institute, Chennai, India for hospitality during a short visit.

References

1. de Broglie, L.: Ph.D. thesis, University of Paris (1924)
2. de Broglie, L.: *J. Phys. Radium* **8**, 225 (1927)
3. Bacciagaluppi, G., Valentini, A.: *Quantum Theory at the Crossroads*. Cambridge University Press, Cambridge (2009)
4. Bohm, D., Hiley, B.J.: *The Undivided Universe*. Routledge, London (1993)
5. Holland, P.: *The Quantum Theory of Motion*. Cambridge University Press, Cambridge (1993)
6. Carroll, R.: *Quantum Theory, Deformation, and Integrability*. North Holland, Amsterdam (2000)
7. Wyatt, R.E.: *Quantum Dynamics with Trajectories: Introduction to Quantum Hydrodynamics*. Springer, New York (2005)
8. Chattaraj, P.K. (ed.): *Quantum Trajectories*. CRC Press, Taylor & Francis, Boca Raton (2011)
9. Floyd, E.R.: Modified potential and Bohm's quantum-mechanical potential. *Phys. Rev. D* **26**, 1339 (1982)
10. Faraggi, A., Matone, M.: Quantum mechanics from an equivalence principle. *Phys. Lett. B* **450**, 34 (1999)
11. John, M.V.: Modified de Broglie-Bohm approach to quantum mechanics. *Found. Phys. Lett.* **15**, 329 (2002)
12. Yang, C.-D.: Quantum dynamics of hydrogen atom in complex space. *Ann. Phys.* **319**, 399 (2005)
13. Yang, C.-D.: Wave-particle duality in complex space. *Ann. Phys.* **319**, 444 (2005)
14. Yang, C.-D.: Modeling quantum harmonic oscillator in complex domain. *Chaos Solitons Fractals* **30**, 342 (2006)
15. Goldfarb, Y., Degani, I., Tannor, D.J.: Bohmian mechanics with complex action: a new trajectory-based formulation of quantum mechanics. *J. Chem. Phys.* **125**, 231103 (2006)
16. Chou, C.-C., Wyatt, R.E.: Computational method for the quantum Hamilton-Jacobi equation: one-dimensional scattering problems. *Phys. Rev. E* **74**, 066702 (2006)
17. Chou, C.-C., Wyatt, R.E.: Computational method for the quantum Hamilton-Jacobi equation: bound states in one-dimension. *J. Chem. Phys.* **125**, 174103 (2007)
18. Sanz, A.S., Miret-Artes, S.: Aspects of nonlocality from a quantum trajectory perspective: a WKB approach to Bohmian mechanics. *Chem. Phys. Lett.* **445**, 350 (2007)
19. Sanz, A.S., Miret-Artes, S.: Comment on "Bohmian mechanics with complex action: a new trajectory-based formulation of quantum mechanics" [*J. Chem. Phys.* **125**, 231103 (2006)]. *J. Chem. Phys.* **127**, 197101 (2007)
20. Goldfarb, Y., Degani, I., Tannor, D.J.: Response to "Comment on 'Bohmian mechanics with complex action: a new trajectory-based formulation of quantum mechanics'" [*J. Chem. Phys.* **127**, 197101 (2007)]. *J. Chem. Phys.* **127**, 197102 (2007)
21. John, M.V.: Probability and complex quantum trajectories. *Ann. Phys.* **324**, 220 (2009)
22. John, M.V.: Probability and complex quantum trajectories: finding the missing links. *Ann. Phys.* **325**, 2132 (2010)
23. Klauder, J.R., Skagerstam, B.: *Coherent States—Applications in Physics and Mathematical Physics*. World Scientific, Singapore (1985)
24. Ali, S.T., Antoine, J.-P., Gazeau, J.-P.: *Coherent States, Wavelets and Their Generalizations*. Springer, New York (2000)
25. Bender, C.M., Boettcher, S., Meisinger, P.N.: PT-Symmetric quantum mechanics. *J. Math. Phys.* **40**, 2201 (1999)
26. Nanayakkara, A.: Classical trajectories of 1D complex non-Hermitian Hamiltonian systems. *J. Phys. A, Math. Gen.* **37**, 4321 (2004)
27. Bender, C.M., Chen, J.-H., Darg, D.W., Milton, K.A.: Classical trajectories for complex Hamiltonians. *J. Phys. A, Math. Gen.* **39**, 4219 (2006)

28. Antoine, J.-P., Gazeau, J.-P., Monceau, P., Klauder, J.R., Penson, K.A.: Temporally stable coherent states for infinite well and Poschl-Teller potentials. *J. Math. Phys.* **42**, 2349 (2001)
29. Bergeron, H., Gazeau, J.-P., Siegl, P., Youssef, A.: Semi-classical behavior of Poschl-Teller coherent states. *Europhys. Lett.* **92**, 60003 (2010)
30. Bergeron, H., Siegl, P., Youssef, A.: New SUSYQM coherent states for Poschl-Teller potentials: a detailed mathematical analysis. *J. Phys. A, Math. Theor.* **454**, 244028 (2012)
31. Rivers, R.J.: Path Integrals for (Complex) Classical and Quantum Mechanics. [arXiv:1202.4117](https://arxiv.org/abs/1202.4117) (2012)